


FRONTIER LETTER

Open Access



Monitoring of equatorial plasma bubbles using aeronautical navigation system: a feasibility study

Keisuke Hosokawa^{1*} , Susumu Saito², Hiroyuki Nakata³, Chien-Hung Lin⁴, Jia-Ting Lin⁴, Pornchai Supnithi⁵, Ichiro Tomizawa¹, Jun Sakai¹, Toru Takahashi², Takuya Tsugawa⁶, Michi Nishioka⁶ and Mamoru Ishii⁶

Abstract

It has long been known that field-aligned irregularities within equatorial plasma bubbles (EPBs) can cause long-range propagation of radio waves in the VHF frequencies such as those used for TV broadcasting through the so-called forward scattering process. However, no attempt has been made to use such anomalous propagations of VHF radio waves for wide-area monitoring of EPBs. In this study, we investigated the feasibility of monitoring of EPBs using VHF radio waves used for aeronautical navigation systems such as VHF Omnidirectional radio Range (VOR). There are 370 VOR stations in the Eastern and Southeastern Asian region that can be potentially used as Tx stations for the observations of anomalous propagation. We have examined the forward scattering conditions of VHF waves using the magnetic field model and confirmed that it is possible to observe the EPB-related anomalous propagation if we set up Rx stations in Okinawa (Japan), Taiwan, and Thailand. During test observations conducted in Okinawa since 2021, no signal has been received that was clearly caused by anomalous propagation due to EPBs. This is simply because EPBs have not developed to high latitudes during the observation period due to the low solar activity. In March 2023, however, possible indications of EPB-related scattering were detected in Okinawa which implies the feasibility of observing EPBs with the current observation system. We plan to conduct pilot observations in Taiwan and Thailand in future to further evaluate the feasibility of this monitoring technique.

Keywords Equatorial plasma bubbles, Radio propagation, Airglow observation

*Correspondence:

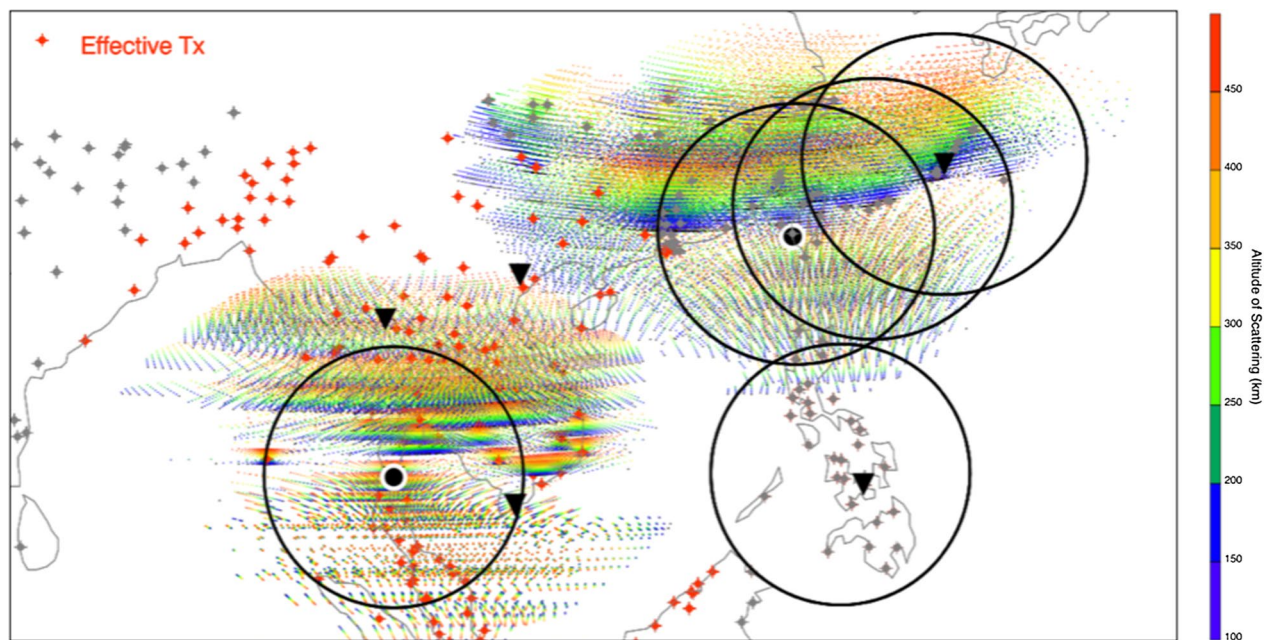
Keisuke Hosokawa
keisuke.hosokawa@uec.ac.jp

Full list of author information is available at the end of the article



© The Author(s) 2023. **Open Access** This article is licensed under a Creative Commons Attribution 4.0 International License, which permits use, sharing, adaptation, distribution and reproduction in any medium or format, as long as you give appropriate credit to the original author(s) and the source, provide a link to the Creative Commons licence, and indicate if changes were made. The images or other third party material in this article are included in the article's Creative Commons licence, unless indicated otherwise in a credit line to the material. If material is not included in the article's Creative Commons licence and your intended use is not permitted by statutory regulation or exceeds the permitted use, you will need to obtain permission directly from the copyright holder. To view a copy of this licence, visit <http://creativecommons.org/licenses/by/4.0/>.

Graphical Abstract



Introduction

Equatorial Plasma bubbles (EPBs) are regions of localized electron density depletion in the F-region ionosphere at equatorial and low latitudes, whose spatial scale ranges from several hundred to several thousand kilometers (as reviewed by Kil 2015 and references therein). EPBs are generated when low-density plasma in the bottom side of the F-region ionosphere is uplifted to higher altitudes, due to the Rayleigh–Taylor-type plasma instability that occurs near the magnetic equator (Woodman and Lahoz 1976). The density depletion within EPBs extends along the magnetic field line; thus, EPBs, that develop toward higher altitudes, can be observed in the low-latitude regions of both the hemispheres 10° – 20° in latitudes away from the magnetic equator (e.g., Otsuka et al. 2002; Shiokawa et al. 2004).

EPBs have been studied extensively by using data from low-altitude satellites and ground-based radio and optical observations. Much has been revealed about the seasonal and longitudinal dependence of their occurrence frequency. For instance, Kil et al. (2009) statistically demonstrated that, in the East Asia, including Japan, and Southeast Asia (around 90° – 150° E), the occurrence frequency of EPBs is high during several hours after the local sunset in equinoctial months. It is also well known that the occurrence rate of EPBs increases during solar maximum periods (Gentile et al. 2006; Kil et al. 2009).

During the solar maximum period around 2000–2004, EPBs were detected at mid-latitudes, for example, at around 30° in geographic latitude over the main land of Japan (e.g., Ogawa et al. 2005; Nakata et al. 2005).

EPBs are known to introduce positioning errors in the Global Navigation Satellite System (GNSS) primarily due to the severe depletion of electron density modifying the phase and group velocities of the navigation signal traveling through the ionosphere. EPBs have also been recognized as one of the primary sources of GNSS scintillations (e.g., Kintner et al. 2007; Bumrungrit et al. 2022; Sousasantos et al. 2022). The amplitude of the navigation signal, propagating through EPBs, often fluctuates due to an interference of radio signals diffracted by plasma density irregularities within EPBs, which sometimes leads to the loss of lock of those signals received on the ground. For these reasons, the impact of EPBs on the infrastructures based on GNSS is apparent, highlighting the relevance of the studies of EPBs in the framework of ionospheric space weather.

The formation mechanism of EPBs, especially the plasma structuring process during the uplift of low-density plasma to higher altitude at the magnetic equator, has rapidly been better understood through recent numerical simulations (c.f. Yokoyama 2017 and references therein). However, the seeding fluctuations required for the Rayleigh–Taylor-type instability to operate are not yet fully

clarified, although several seeding mechanisms have been proposed such as large-scale wave structures (e.g., Tsunoda 2015 and references therein) and modulation by upward-propagating gravity waves (e.g., Huang and Kelley 1996). This has made it still difficult to precisely predict the day-to-day variability of EPBs even by employing recent numerical models (e.g., Carter et al. 2014; Shinagawa et al. 2018). For this reason, it is still required to monitor the occurrence of EPBs and EPB-related GNSS scintillations in a wide area for the stable use of GNSS-based navigation.

EPBs have been measured by several observational techniques from the ground such as 630.0 nm airglow imagers (Weber et al. 1978; Otsuka et al. 2002), coherent radars at VHF frequencies (Fukao et al. 2003; Otsuka et al. 2009), GNSS total electron content observations including GNSS-ROTI (e.g., Buhari et al. 2017), and anomalous propagation of trans-equatorial HF waves (Röttger 1976; Maruyama and Kawamura 2006; Saito et al. 2018). However, a combination of multiple methods is indispensable for more redundant monitoring in a wide area because each of these methods has its own advantages and disadvantages. Thus, the establishment of a new observation method has still been highly demanded.

As one of such new methods for monitoring EPBs, Nakata et al. (2005) demonstrated that EPBs can be detected by using a long-range anomalous propagation of VHF radio waves. They reported that their VHF receiver in Tateyama, Japan often observed signal intensity increases at several frequencies between 50 and 73 MHz for several hours after the local sunset during equinoctial months. The source of one of those signals at 59.75 MHz was identified to be a TV broadcasting station in Manila, Philippines, which is more than 4000 km away from the receiving station. They performed a ray tracing of this TV broadcasting radio by considering the forward scattering due to the EPB-related irregularities and suggested that the area of scattering was distributed in the southwestern part of Japan. It was also confirmed that, in some cases, EPBs were actually observed by an all-sky airglow imager near the estimated area of scattering during intervals of anomalous propagation. Based on the results of above-mentioned analyses, Nakata et al. (2005) concluded that EPBs were the agent causing such anomalous long-range propagation of VHF radio; thus, passive measurements of VHF radio waves can be used for monitoring the appearance of EPBs. However, the number of TV broadcasting stations is insufficient for establishing a network observation aiming at routine monitoring of EPBs. In addition, it is not always possible to identify the transmitting source stations for mapping the location of scattering (i.e., the location of EPBs).

To overcome these limitations, this paper proposes to employ VHF radio waves used for aeronautical navigation (air navigation) system for wide-area monitoring of EPBs. The advantages of using aeronautical navigation radios are as follows: (1) location of radio transmission, transmission frequency, and operation schedule are publicly available; (2) it is possible to identify the source station from the identification code obtained by decoding the modulation of the signal. We have used such air navigation radio waves to detect the appearance of sporadic E that occurs at mid-latitudes during summer months (Sakai et al. 2019). The observation system continuously records the signal intensity of air navigation signals (VOR, ILS-LOC) in 108–118 MHz frequency range using a software receiver (Hosokawa et al. 2020a). When sporadic E appears at around 100 km altitudes, VHF radio waves incident obliquely into the ionosphere are reflected by sporadic E and propagate over long distances. By detecting such cases of long-range anomalous propagation at several receiving stations, the geolocation of sporadic E can be mapped at an intermediate point between the transmitting and receiving stations (Sakai et al. 2020). Currently, the observation system is in operation at seven sites in Japan, and, in combination with GPS total electron content observations, the spatial extent of sporadic E has been visualized in a two-dimensional fashion (Hosokawa et al. 2021).

In this paper, we conducted a feasibility study of EPB monitoring using VHF radios for the aeronautical navigation system. In particular, we evaluated the feasibility of wide-area observations of EPBs by carrying out ray-tracing calculation of the forward scattering process as well as by conducting pilot observations in Okinawa, Japan. When conducting the ray tracing, we assumed several imaginary receiving stations in the eastern and southeastern Asia with the actual distributions of transmitting stations of aeronautical navigation system, which allows us to plan for constructing a network observation in an efficient way. In the pilot observation, we compare the radio observation with all-sky airglow observations (Hosokawa et al. 2020b) and GNSS scintillation measurements of EPBs in Ishigaki Island, Japan.

Methods

In this paper, we propose a method for detecting EPBs by using passive observations of VHF omnidirectional radio range (VOR) which is broadcasted from a number of ground-based stations (at airports in most cases) at VHF frequencies from 108 to 118 MHz. If the transmitted radio is forward scattered by EPBs and propagates for a long distance, the reception of such signals at a distant location would be used for detecting EPBs along the ray

path of the radio. In particular, it would be possible to estimate the possible location of EPBs (i.e., the location of EPB-related scattering) by combining the radio measurements in several places with calculation of scattered ray path as demonstrated by Nakata et al. (2005).

First, to evaluate the feasibility of the proposed method, we have performed a simple ray-path calculation including the forward scattering by plasma irregularities associated with EPBs. Plasma irregularities are known to have a structure perpendicular to the local magnetic field lines owing to the high mobility of plasmas along the field. In addition, high aspect sensitivity is expected for the scattering by the EPB-related irregularities (e.g., Stathacopoulos and Barry 1974; Rao and Thome 1974). As such, when radio waves are incident on the EPB-related irregularities, strong forward scattering occurs in directions where the reflection angle is equal to the incident angle, which is known as the Bragg scattering condition. Thus, the scattered rays should be on the surface of a cone whose half-angle coincides with the angle between the

incident wave and the local magnetic field. By tracing the ray paths on this cone of strong forward scattering, we could extract successful rays propagating all the way from the source transmitting (Tx) stations to the receiving (Rx) stations.

When conducting the calculation, first we define the Tx and Rx stations. Then, we consider radio waves that are transmitted in all the azimuthal angles (0–360 degrees, every 5 degrees) and elevation angles (0–90 degrees, every 1 degree). For these radio waves, we evaluate the scattering condition along the ray path and check if the scattered radio wave can reach Rx. When checking the scattering condition, a magnetic field model of the IGRF-12 (International Geomagnetic Reference Field, IGRF-12: Thebault et al. 2015) is used to obtain the vector of the local magnetic field at each point in the ionosphere. We also assume the straight-line propagation (i.e., without refraction) since now we consider radio waves in VHF frequency above 100 MHz.

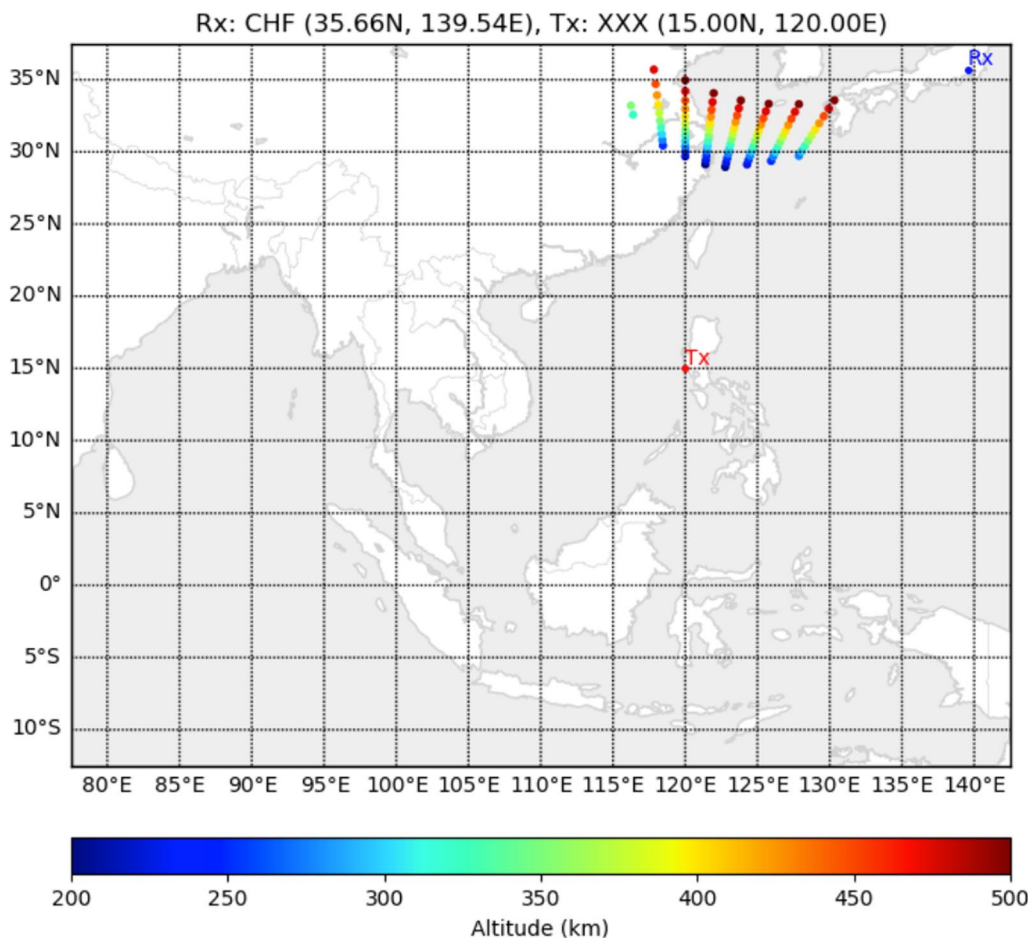


Fig. 1 An example of the calculation of scattering condition. The Tx station is in Manila, Philippines and the Rx station is in Tokyo, which is very close to Chiba

An example of the calculation is shown in Fig. 1 where the possible locations of forward scattering are displayed as colored circles. This example aims at reproducing the scattering condition of Nakata et al. (2005) using the same Tx and Rx. That is, the Tx station is in Manila, Philippines and the Rx station is in Tokyo, which is very close to Chiba. The color of the points indicates the altitude of scattering. The orthogonality between the ray and the local magnetic field determines the dependence of the location of scattering on altitude. In the current case, the orthogonal condition is satisfied at higher altitudes in higher latitudes. Although the locations of the scattering points vary slightly with altitude, all the scattering points are distributed in the western part of Kyushu, which is in agreement with the estimation by Nakata et al. (2005). This indicates that the assumption of straight-line propagation and the use of the IGRF model is able to reproduce the scattering conditions at VHF frequencies.

We conduct the calculation of scattering condition by using the actual locations of VOR stations at low latitudes in the Asian and Oceanian regions. Those source VOR stations will be used as Tx stations for the actual monitoring observations. We have used a list of VOR stations available at <https://ourairports.com> and published in the CSV format (<https://ourairports.com/data/navaid.csv>), and then listed up 370 stations in the area within the fields of view of the possible Rx stations (70° – 140° E in longitude and 10° S– 30° N in latitude). The Tx stations in the list may change in time; thus, updated list of VOR stations should be verified with the official Aeronautical Information Publication (AIP) when we analyze the data in detail. Those VOR stations are plotted in Fig. 2 by the red dots with cross. When conducting the calculation, we considered the five imaginary receiving (Rx) stations, that are Chofu, Tokyo (CHF), Kure, Hiroshima (KUR), Onna, Okinawa (ONA), Tainan, Taiwan (TAN), and Chumphon, Thailand (CPN), which are also indicated by the black large dots in Fig. 2.

At the three Rx stations in Japan (CHF, KUR, ONA), monitoring system of aeronautical navigation radio has already been operative for observing the sporadic E. The receiving system consists of a software-defined receiver, a small PC, and a log-periodic antenna and observes the frequency spectrum of VHF radio waves from 98 to 118 MHz in a continuous manner (Hosokawa et al. 2021). The systems at these three stations are not equipped with an amplifier, attenuator, and air band filter before the signal processing at the software-defined receiver. At the Rx station in Onna, Okinawa, it is possible to carry out test observations by directing the antenna toward southeast, which is currently pointed toward the north to observe the sporadic E over Japan. As shown in Fig. 2, ionosondes operated by the National Institute of Information and

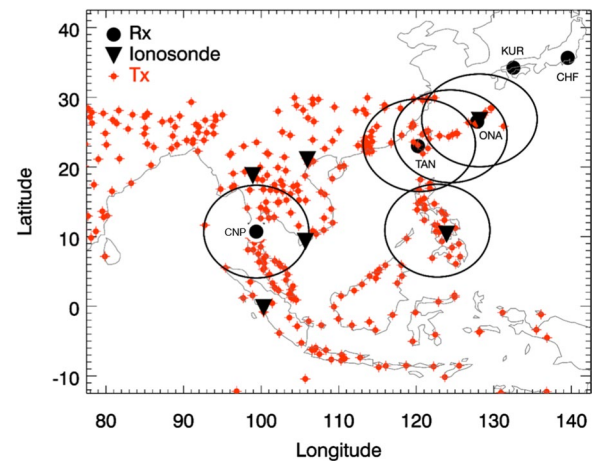


Fig. 2 Distribution of the Rx (black large dots) and Tx (red dots with cross) stations. The black open circles show the fields of view of the 630.0 nm all-sky airglow imager

Communications Technology (NICT) are able to detect the spread F signatures in ionograms during EPBs. The five large circles in Fig. 2 indicate the fields of view of the 630.0 nm all-sky airglow imagers (Hosokawa et al. 2020b), which can also be used for detecting the appearance of EPBs in the region of interest.

Results

Figure 3 shows the results of calculations of the scattering conditions based on the actual distribution of Tx stations in Fig. 2. In Fig. 3a, the distribution of all the 370 Tx stations is plotted again by the gray dots with cross. The remaining five panels display the distributions of scattering points for five different locations of Rx station, which are CHF, KUR, ONA, TAN, and CPN, respectively. The color of the points again indicates the altitude of scattering. The Tx stations are plotted by the red or gray dots with cross, where the radio waves from the red dots are received at the Rx station, while those from the gray dots do not reach the Rx station. An additional note is that the scattering points plotted here are only those where the propagation distance between the Tx and Rx stations is less than 4000 km. This distance of 4000 km is taken from the results of Nakata et al. (2005) where the distance from the Tx station in Philippines and the Rx station in Chiba, Japan was roughly 4000 km.

Figure 3b–f demonstrates that the closer the receiving point is to the equator, the more scattering points are distributed in the low-latitude region where the occurrence of EPBs is generally higher. Figure 3b, c indicates that most of the possible scattering points are distributed at latitudes above 30° N when the Rx station is located in the mainland of Japan (CHF and KUR). Nakata et al. (2005) implied that EPBs can be observed by their VHF

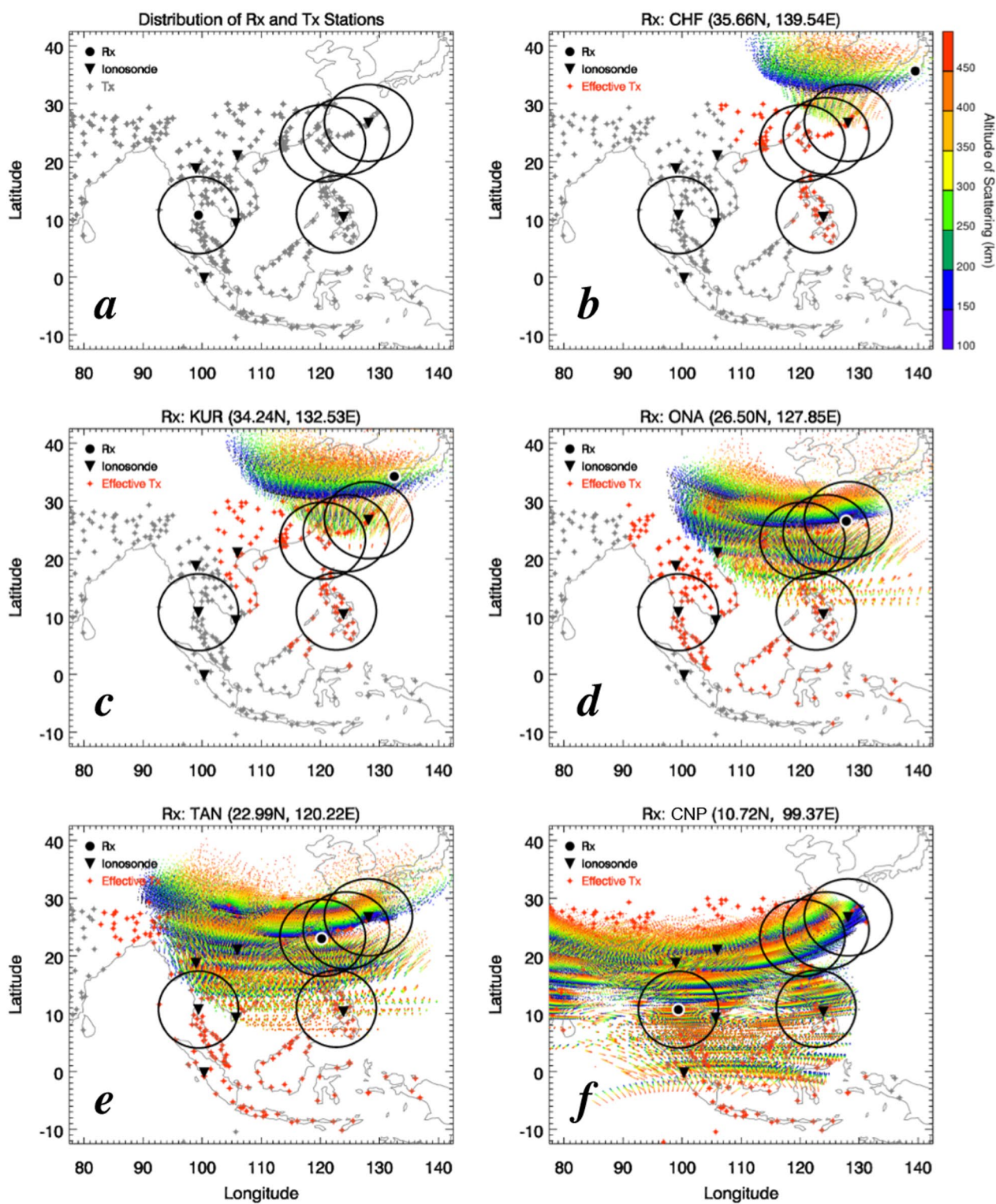


Fig. 3 Results of calculation of scattering points where the color indicates the altitude of scattering: **a** distribution of Tx stations, distribution of scattering points for **b** CHF, **c** KUR, **d** ONA, **e** TAN, and **f** CNP

radio monitoring system in Japan only during a few years near the peak of the solar cycle 23. Since then, the solar activity has been lower than that even during the solar maximum period; thus, it would be difficult to detect EPB-related long-range propagation of VHF waves by receivers in the mainland of Japan.

Figure 3d, e shows the results of the calculations for the cases of Rx station in Okinawa (ONA) and Tainan (TAN), respectively. Although there is a slight difference in the distribution between the two cases, the scattering points are distributed in a large area covering latitudes from 10 to 30°N, indicating that the detection of EPBs is expected if they develop to the southern islandic area of Japan, Taiwan, southern China, and northern Southeast Asia. The result of the case where the Rx station is located further south in Chumphon, Thailand (CPN) is shown in Fig. 3f. In this case, the scattering points are distributed over a further wide area in both the latitude and longitude because the Tx stations are located in all directions from the Rx station. In addition, since the Rx station is located near the magnetic equator, it is expected to receive the EPB-related scattering from both the northern and southern sides of the magnetic equator. The other thing worth noting is that the scattering points for the cases of Rx stations at ONA, TAN, and CPN are distributed well within the fields of view of the all-sky airglow imagers indicated by the large circles. This will allow us to verify whether the anomalous propagation of aeronautical navigation radios, if received, are surely caused by EPBs or not.

Figure 4 shows the results of the same calculation, but here we only consider scattering of radio waves from Tx stations within 2000 km propagation distance from the Rx station. Figure 4b, c again indicates that scattering points do not cover the area where EPBs are expected to be observed when the monitoring system is deployed in the main land of Japan (the latitude of sensing area is higher than 30° in these cases).

On the other hand, if the Rx stations are located at lower latitudes such as Okinawa (Fig. 4d) and Tainan (Fig. 4e), the scattering points were found to be distributed over a wide area from 10° to 30° geographic latitudes (roughly 0°–20° degrees in magnetic latitude). This covers a wide area including Ishigaki, Taiwan, and the northern part of Southeast Asia. Several cases of EPBs were detected by all-sky airglow imagers in Ishigaki (Hosokawa et al. 2021) and Tainan (Rajesh et al. 2017) during the peak of the previous solar maximum (the solar cycle 24); thus, we could expect to verify the feasibility of the proposed method by conducting simultaneous observations with the optical instruments in this. As shown in Fig. 4d, e, most of the radio signals, that can be received in Okinawa and Tainan, propagated from the southern

and western part of the Rx stations; thus, the receiving antenna in these Rx stations should be directed to the southwest.

Figure 4f again shows that it is possible to receive scattered radio waves from all directions if the observation is made at Chumphon, Thailand. We plan to use the log-periodic antenna (CLP5130-2), having a wide directivity with a 3 dB beam width of 60 degrees in the azimuthal direction. Thus, it is considered appropriate to install the antenna pointing directly upward to receive radio waves from a wider direction. In this case, we expect to receive signals from the Philippines from the east and those from India from the west at the same time, allowing us to monitor EPBs over a wider area if the strength of the received signal is sufficiently high.

Comparing the results of these two calculations shown in Figs. 3 and 4, the spatial extent of the scattering points, which is identical to the coverage of the monitoring, is more limited in the case of the 2000 km propagation distance (Fig. 4). Even for this case, however, the sensing area would cover a large area in the low-latitude and equatorial regions. Figure 5a shows the combined distribution of the scattering points for all the three low-latitude Rx stations (Okinawa, Tainan, and Chumphon). The scattering points are distributed in a wide area extending from the southeastern Asia to the low-latitude part of the eastern Asia.

Discussion

In this study, based on the observations of Nakata et al. (2005), we examined the feasibility of using the anomalous long-distance propagation of aeronautical navigation radios for detecting EPBs. The calculation of scattering condition demonstrated that it would be possible to detect EPBs in a wide area at low latitudes if we set up a few Rx stations in the eastern and southeastern Asia. This is primarily because the number of usable Tx stations (VOR stations) is very large, ~370 stations in the region of interest. Still, however, there are a few things that have not been taken into account in the feasibility study introduced in the previous section.

First is the frequency dependence of the Bragg scattering process. Nakata et al. (2005) employed TV broadcast radio waves with a frequency of about 60 MHz, whereas the current method uses aeronautical navigation radio waves in the 108–118 MHz frequency band. Considering the Bragg scattering mechanism, the spatial scale of plasma irregularities should be shorter for the case of higher frequency of the incident wave. In general, the amplitude of the irregularities decreases as their spatial scale becomes smaller; thus, the intensity of the scattered waves is expected to be smaller for the case of aeronautical navigation radio. Kuriki

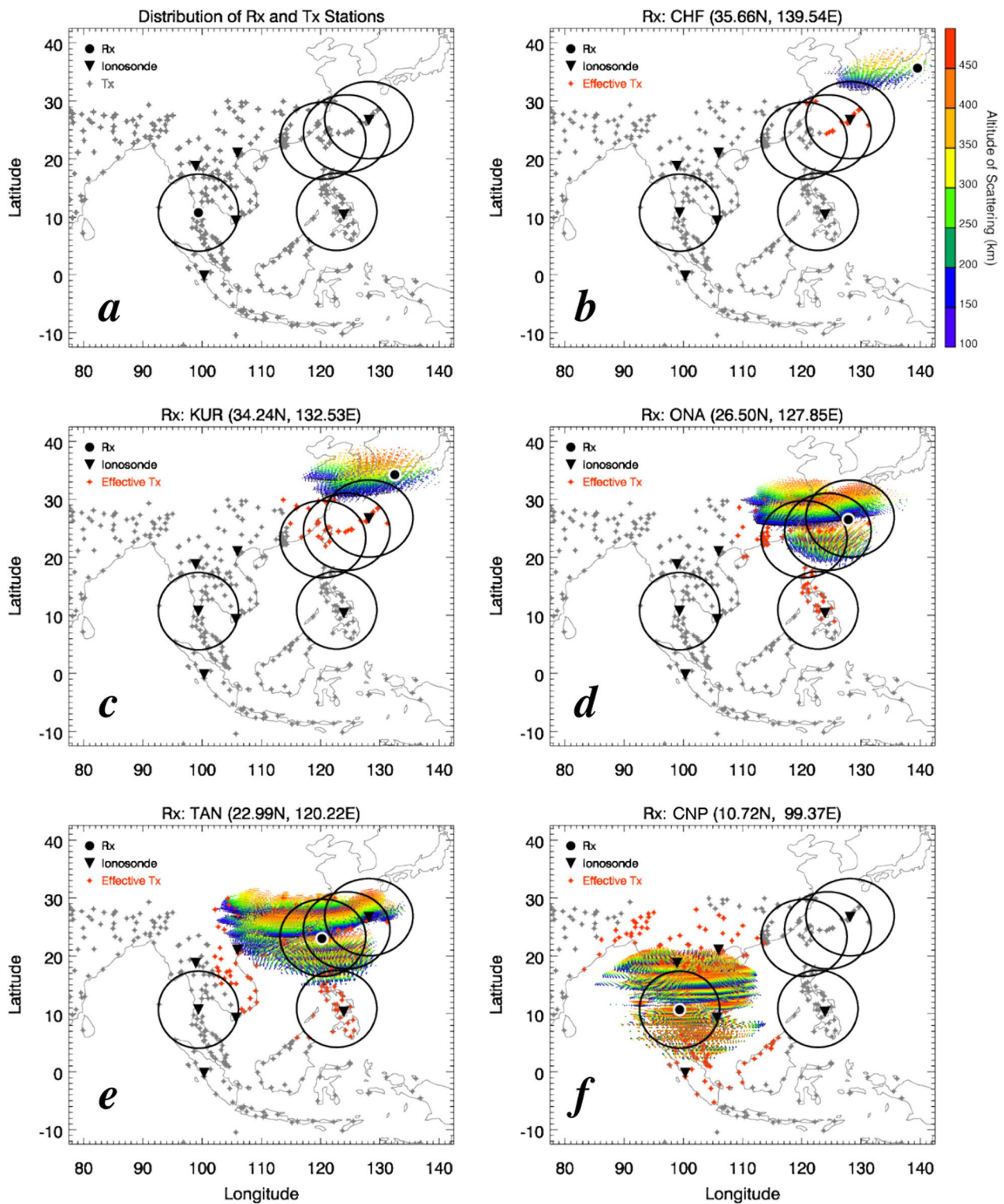


Fig. 4 Results of calculation of scattering points. The format is same as Fig. 3, but here only rays of propagation distance less than 2000 km are considered: **a** distribution of Tx stations, distribution of scattering points for **b** CHF, **c** KUR, **d** ONA, **e** TAN, and **f** CNP

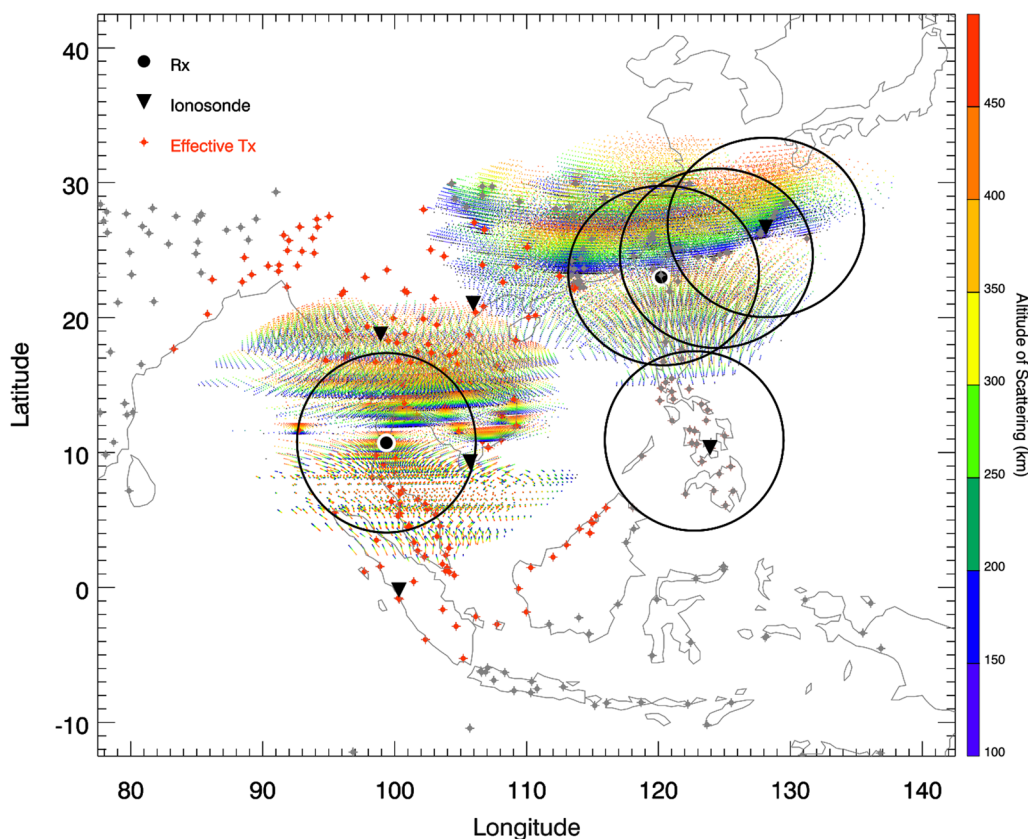


Fig. 5 Combined distribution of the scattering points for all the three low-latitude stations (Okinawa, Tainan, and Chumphon)

et al. (1972) estimated the frequency dependence of the received signal intensity of trans-equatorial propagation of VHF radio waves possibly scattered by EPBs and implied that the received signal intensity is proportional to f^{-5} in the case of single scattering propagation. Following this estimation with the frequencies used by Nakata et al. (2005), that is around 60 MHz, and the current method (110 MHz), the signal intensity that we expect to obtain would be ~12 dB lower than that of Nakata et al. (2005). In addition, the spatial attenuation of radio waves in the atmosphere tends to increase as the frequency increases. It is difficult to evaluate how much these factors will actually affect the observations based only on the theoretical estimates; thus, actual observations at low latitudes are required to further discuss these points.

The actual observability also depends on the propagation distance of radio waves. Nakata et al. (2005) used TV broadcast signals having a few tens of kW transmission power. In contrast, most VOR stations transmit the signal with power of 200 W, which is approximately 20 dBm lower than that of the TV broadcast stations. In addition, the receiving system used by Nakata et al. (2005) was equipped with a 10 dB amplifier; thus, the signal level of

the current observation system should be ~30 dB lower than that of Nakata et al. (2005). However, in the case shown in Nakata et al. (2005), the signal intensity of the EPB-related signals was often ~50 dB higher than the background level. Given this margin, we consider it possible to receive the aeronautical navigation radios with a sufficient S/N ratio relative to the background even when the transmission power is ~30 dB lower than the TV station case and ~12 dB power penalty is introduced by the use of higher frequency. In Nakata et al. (2005), radio waves were received with the sufficient margin even when the propagation distance was about 4000 km. Since we could use a number of VOR stations within much closer distances, it is conceivable that signal reception will be possible particularly at shorter propagation distances, if the same measurement system as Nakata et al. (2005) is used.

Assuming that anomalous propagation due to EPBs can be observed at the Rx stations, it is necessary, as a next step, to identify the source Tx stations in order to identify the location of EPBs responsible for the scattering. In general, VOR stations within the range of direct propagation do not use the same frequency channel. However, since the distance of anomalous propagation sometimes

exceeds 1000 km, there may be multiple candidate Tx stations corresponding to the frequency at which the anomalous propagation is detected. In such a case, it is rather difficult to determine the source Tx station from the frequency allocation information alone. When visualizing the spatial distribution of sporadic E using anomalous propagation, the midpoints between all candidate Tx and Rx stations (i.e., locations of reflection due to sporadic E) are plotted on the map, and then, the true reflection points (i.e., the true location of Es) are extracted by considering the concentration of the candidate points (Hosokawa et al. 2021).

By checking the frequency channels assigned to the 370 VOR Tx stations listed in Fig. 1, we found that ~10 stations use the same frequency. Considering the 114.30 MHz frequency channel as an example, 11 stations out of 370 use the same frequency. When the receiving point is in Okinawa, 8 out of the 11 stations are located within propagation distance of 4000 km. When the distance of propagation is limited to 2000 km, the number of candidate stations is reduced to 2. In such a case, mapping of all possible candidate scattering points for multiple frequency channels would allow us to identify the true scattering point from the concentration of the candidate points. We plan to verify the feasibility of this mapping technique by applying it to actual cases of anomalous propagation due to EPBs.

In parallel with the theoretical estimation of the scattering conditions, we have carried out test observations in Okinawa during the fall months of 2021. The receiver in Okinawa is normally used for observing sporadic E by pointing the antenna to northeast to cover the E region ionosphere over Japan. During the testing, we directed the antenna to southwest to detect anomalously scattered aeronautical navigation radios from the low-latitude region. Following an increase of solar activity in the summer of 2021, several EPBs were observed by the 630.0 nm all-sky optical imager in Ishigaki Island during 3 months from September to November 2021. 15 cases of EPBs were observed during periods after the sunset and before the midnight (11–15 UT in Ishigaki).

Here, we introduce two EPB events observed respectively on the consecutive nights of October 31 and November 1. In the snapshots of 630.0 nm all-sky airglow images in Fig. 6a, b, EPBs are seen as dark tree-like regions of reduced airglow intensity extending beyond the zenith of Ishigaki Island. Assuming the emission altitude of 630.0 nm airglow emission to be 250 km, the EPBs are considered to have extended to about 27° in latitude. Figure 6c, d shows the S4 index from a GNSS scintillation receiver in Ishigaki Island. The amplitude scintillation related to EPBs was detected in the southern part of the all-sky field of view. However, the S4 index

did not increase much in the northern side of the zenith, suggesting that the plasma irregularities, that can cause anomalous propagation, occurred only at lower latitudes than the latitude of the EPBs themselves. It is noted that the all-sky images have been flipped in the horizontal direction for easier comparison with the GNSS scintillation measurement.

Figure 7 shows the observations of aeronautical navigation radio waves in Okinawa on October 31 and November 1. The data are shown in a format of dynamic spectra where the lower panels (Fig. 7b, d) correspond to the broadcasting band from 98 to 108 MHz and the upper panels (Fig. 7a, c) to the aeronautical navigation band from 108 to 118 MHz. The periods, during which EPBs were detected in Ishigaki Island in the south of Okinawa, are indicated by the red boxes. Nakata et al. (2005) demonstrated that increases of the signal intensity were seen at multiple frequencies during the interval of EPB-related anomalous propagation. Here, however, no clear signs of such enhancements are seen in the spectra during the interval of EPBs. As mentioned above, we have identified 15 cases of EPBs in the airglow data during the autumn in 2021 although most of them were seen in regions very close to southern horizon. For all the 15 cases, we did not find any clear signatures of EPB-related scattering as shown in the representative cases in Fig. 7.

There are at least three possible reasons for the absence of EPB-related scattering during the test observations: (1) the positional relationship between the radio wave path and the EPBs was not suitable for receiving scattered waves, (2) the intensity of the scattered waves was insufficient to be received in Okinawa since the possible source Tx stations were mostly located in the southeastern Asia which is far from the Rx station, and (3) plasma irregularities, responsible for the scattering of radio waves, may not have reached to high latitudes, i.e., to the coverage of measurement in Okinawa. Another cause may be that we have used a receiving system different from the one of Nakata et al. (2005). Evaluation of the difference in sensitivities between those systems using data of actual anomalous propagation is required when we obtain actual cases of anomalous propagation due to EPBs.

As described in this section, we were unable to receive any signals that could be reliably concluded to be the signatures of the long-range anomaly propagation associated with EPBs during the autumn season of 2021. Considering that the all-sky airglow imager in Ishigaki observed 15 cases of EPBs during the same period, it is conceivable that the observation in Okinawa would be difficult to receive signals at least during solar minimum. At the time of the test observation, the solar activity has not yet reached its maximum; thus, there have been few

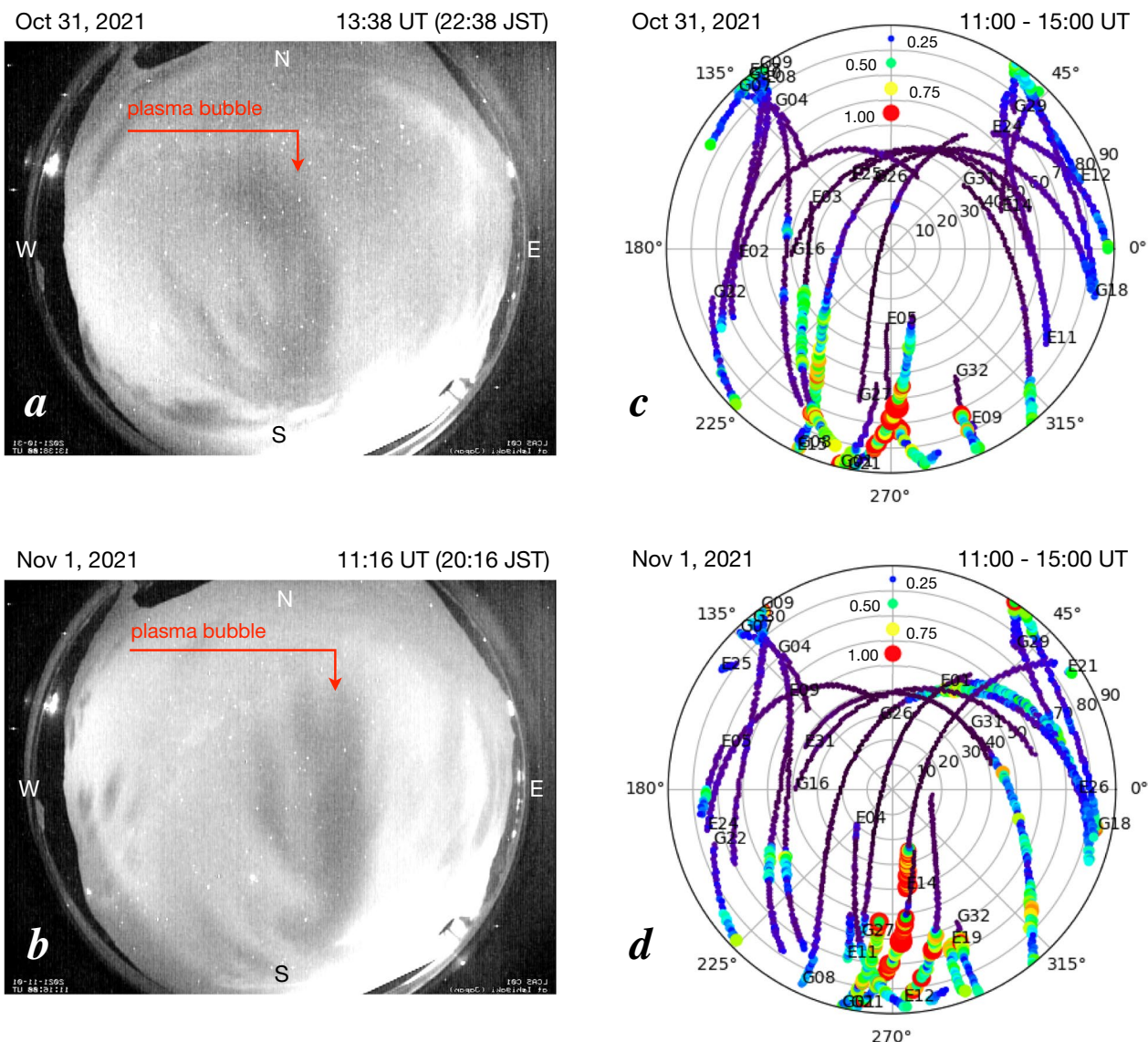


Fig. 6 **a, b** 630.0 nm all-sky images obtained from Ishigaki Island, respectively, on the nights of Oct 31 and November 1, 2021. **c, d** S4 index obtained from a GNSS receiver in Ishigaki on the nights of Oct 31, and November 1, 2021

cases (only two during the observation period) in which EPBs have fully developed to the possible scattering area (i.e., the field of view) that would be expected if observations were made in Okinawa.

In March 2023, possible signatures of EPB scattering were identified in Okinawa only in the broadcasting band from 98 to 108 MHz, one of which is summarized in Fig. 8. In Fig. 8b, enhancements of the received signal intensity can be recognized in the broadcasting band as indicated by the red arrows. No corresponding enhancement was seen in the aeronautical navigation band from 108 to 118 MHz (Fig. 8a). These enhancements occurred at around 01 JST on March 17, 2023 (16 UT on March

16, 2023), during which optical signatures of EPB were captured by the all-sky airglow imager in Ishigaki as displayed in Fig. 8c. Although this signature of EPB-related scattering was brief, whose duration was ~15 min, the received signal intensity increased at multiple frequency channels, which is very similar to the signature reported by Nakata et al. (2005).

It is rather difficult to provide definitive evidences confirming that the enhancements in the received signal intensity during this case is surely associated with EPBs. However, before showing this particular case, we have discarded many cases of signal intensity enhancement in Okinawa. Most of them are related to the so-called

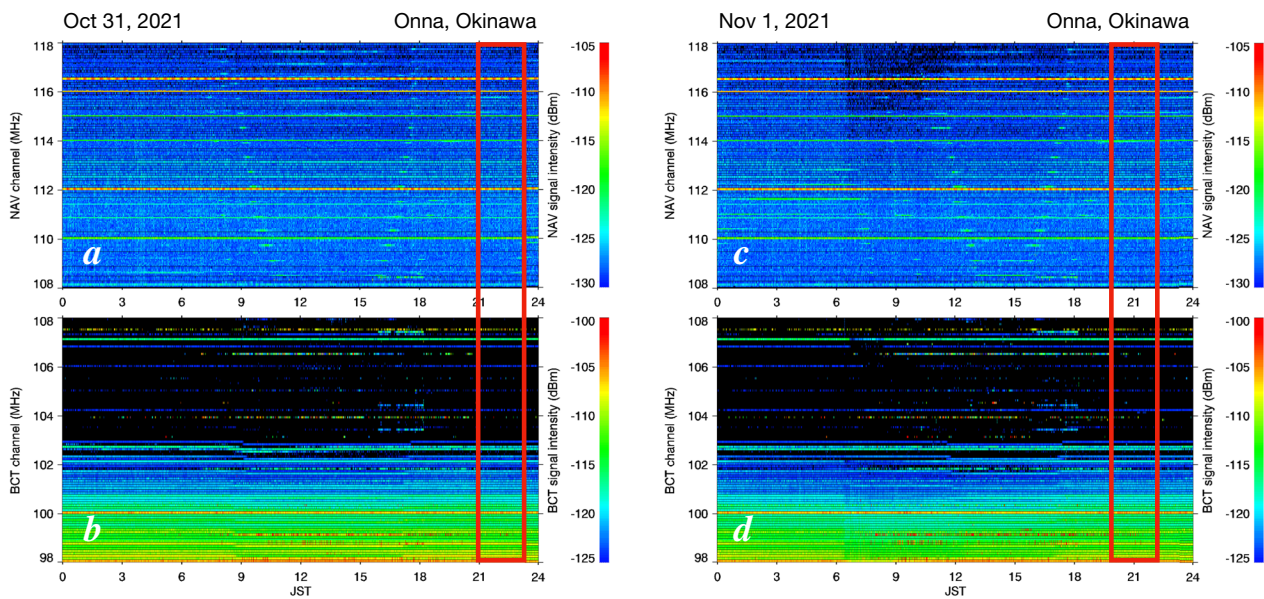


Fig. 7 Observation of VHF radio observation in Okinawa on Oct 31 (a, b), and November 1 (c, d), 2021. The upper panels (a, c) are the dynamic spectra of received signal intensity in the aeronautical navigation band from 108 to 118 MHz, while the lower panels (b, d) are those in the broadcasting band from 98 to 108 MHz

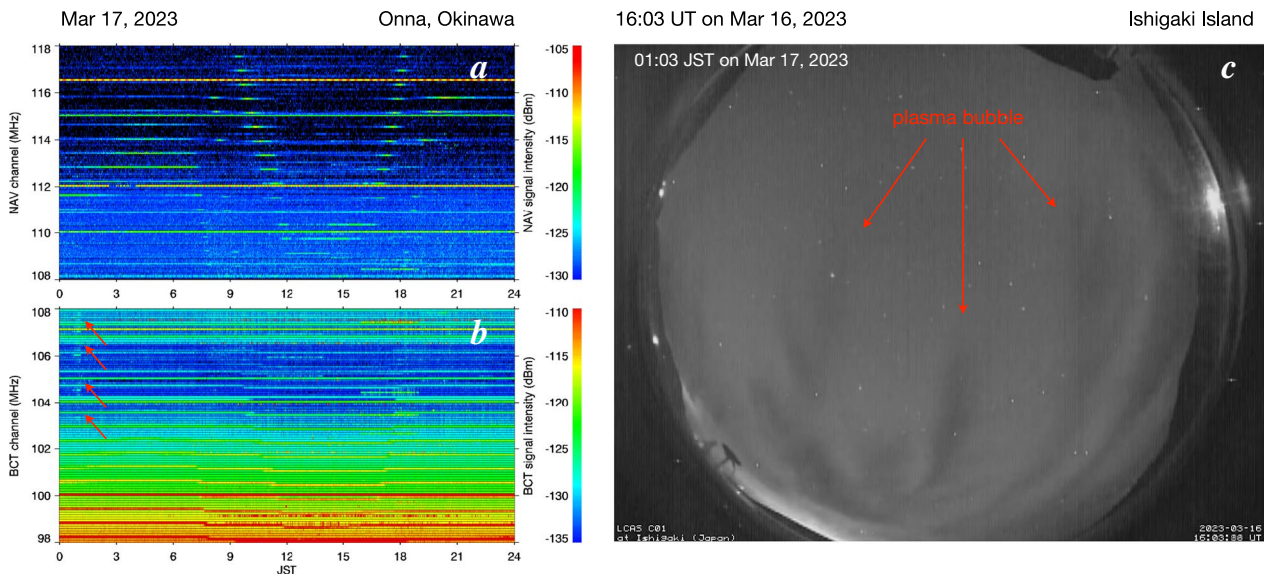


Fig. 8 Observation of VHF radio observation in Okinawa and optical observation in Ishigaki on March 17, 2023. **a** The dynamic spectra of received signal intensity in the aeronautical navigation band from 108 to 118 MHz, **b** the dynamic spectra of received signal intensity in the broadcasting band from 98 to 108 MHz where the possible signatures of EPB scattering are indicated by the red arrows, **c** 630.0 nm all-sky images obtained from Ishigaki Island at 16:03 UT on March 16, 2023 (01:03 JST on March 17, 2023) in which multiple traces of airglow depletion associated with EPBs are seen

tropospheric ducted propagation, which can occur even during the daytime. In contrast to tropospheric ducted propagation, EPB-related scattering occurs only after the sunset. Such a local time dependence of the occurrence

timing is one of the points supporting the current interpretation. We also considered a similarity with anomalous propagations caused by the sporadic E layer (e.g., Sakai et al. 2019; Hosokawa et al. 2020a, b). The signal

enhancement due to the sporadic E tends to occur at multiple frequency channels, sometimes extending the entire frequency range from 98 to 118 MHz. In the current case, the enhancements were seen at multiple frequency range at least in the broadcasting channel, which is another point supporting our interpretation.

We are not able to determine which trace of EPBs in Fig. 8c was responsible for the scattering causing anomalous propagation. This would be one of the shortcomings of the current observation method. Instead of this weakness, however, the current method has an advantage in monitoring the occurrence of EPBs in a wide area. Regarding the absence of signal enhancement in the aeronautical navigation band above 108 MHz, one of the possible reasons is the difference in the transmitting power of the Tx station. In general, the transmitting power is much higher in the broadcasting channel than in the aeronautical navigation channel. The difference between the aeronautical (Fig. 8a) and broadcasting (Fig. 8b) bands should have been primarily caused by this difference in the power of the source Tx station.

The scale size of EPBs during a few cases in 2021 introduced in Fig. 6 is slightly larger than that seen in the current case in 2023. One of the factors controlling the "general" occurrence of anomalous propagation is the latitude of EPBs. At the same time, the occurrence of anomalous propagation depends on the spatial relationship between the locations of EPBs and Tx/Rx stations (i.e., ray path). This might have allowed us to detect the possible signature of EPB-related anomalous propagation even during a relatively smaller-scale EPBs. The other difference between the EPBs in Figs. 6 and 8 is the local time of their occurrence, i.e., the EPBs in Fig. 6 occurred well before the midnight, while the ones in Fig. 8 were observed slightly after the midnight. The background electron density in the F region should have been lower after the midnight (Fig. 8) than that before the midnight (Fig. 6) which might also have introduced the difference in the occurrence of anomalous propagation between the EPB events in Figs. 6 and 8.

This implies the feasibility of detecting EPB scattering using passive observations of VHF radio waves at around or above 100 MHz. We have started observation in Tainan, Taiwan just recently and will deploy an additional receiver in Thailand in 2023. Those new observations at lower latitudes will be used for further evaluating the feasibility of the current method for observing EPBs in a wide area.

Summary and conclusion

We proposed a method to observe EPBs using the scattering and resultant long-range propagation of radio waves used for aeronautical navigation system at VHF frequencies. We have theoretically verified the conditions

of Bragg scattering due to EPBs and carried out test observations in Okinawa, Japan. The results are summarized as follows:

- There are 370 VOR stations in the equatorial/low-latitude region of the Asian sector (70–140°E in longitude and 10°S–30°N in latitude). Those stations can potentially be used as the source Tx stations for the long-range propagation when a receiving point is set up in East and Southeast Asia. Of these stations, 11 stations at most use the same frequency channel. In order to derive the spatial distribution of EPBs using this observation method, it is necessary to establish a method to identify the source Tx station by combining the current measurement with the ray-tracing calculation, especially when radio waves using the same frequency channel are observed simultaneously.
- The calculation of radio wave scattering conditions using the magnetic field model confirmed the possibility of EPB-related scattering when receiving points are located in Okinawa, Taiwan, and Thailand. On the other hand, when receivers are located in the mainland of Japan, the scattering points were not distributed in the low-latitude and equatorial regions where EPBs are expected to reach during the solar minimum.
- Test observations were conducted in Okinawa, Japan in the autumn months in 2021, but signals, that are clearly attributed to EPB-related scattering, were not received. This is simply because EPBs have not developed to higher latitudes during the previous solar minimum period, i.e., up to the possible sensing area of the test observation. In March 2023, however, possible signatures of EPB-related scattering were identified in the broadcasting band from 98 to 108 MHz, which implies the feasibility of monitoring the appearance of EPB using the VHF radio observations. We plan to start continuous observations in Taiwan and Thailand to further demonstrate the feasibility of our observation method during the coming solar maximum period.
- The intensity of scattered signal may be relatively small even when they are observed at the Rx stations. This is primarily because the frequency of the aeronautical navigation radio is higher than that of previous studies using TV broadcast radio waves at about 60 MHz and the transmission power is lower than that of the TV broadcast radio. This will be evaluated based on the results of observations in the south, which are planned to be conducted soon.

Abbreviations

EPBs	Equatorial plasma bubbles
GNSS	Global navigation satellite system
ROTI	Rate of TEC Index
GPS	Global positioning system
IGRF	International Geomagnetic Reference Field
JST	Japan standard time
NICT	National Institute of Information and Communication Technology
TEC	Total electron content
UT	Universal time
VHF	Very high frequency
VOR	VHF omnidirectional radio range

Acknowledgements

KH thanks A. Nadai and M. Oshiro at the Okinawa Electromagnetic Technology Center of National Institute of Information and Communications Technology for supporting the VHF radio observation at Onna, Okinawa.

Funding

This work was supported by the collaboration research project of Electric Navigation Research Institute (ENRI).

Availability of data and materials

Data of VHF radio observations in Okinawa introduced in this paper are available upon request (contact: Keisuke Hosokawa). Data of the airglow imager and GNSS scintillation measurements from Ishigaki Island are also available upon request (contact: Keisuke Hosokawa and Susumu Saito).

Declarations

Ethics approval and consent to participate

Not applicable.

Consent for publication

Not applicable.

Competing interests

The authors declare that they have no competing interests.

Author details

¹Center for Space Science and Radio Engineering, University of Electro-Communications, Chofugaoka 1-5-1, Chofu, Tokyo 182-8585, Japan. ²Electronic Navigation Research Institute, National Institute of Maritime, Port and Aviation Technology, Jindajji-Higashicho 7-42-23, Chofu, Tokyo 182-0012, Japan. ³Graduate School of Engineering, Chiba University, Chiba, Japan. ⁴Department of Earth Sciences, National Cheng Kung University, Tainan, Taiwan. ⁵School of Engineering, King Mongkuts Institute of Technology Ladkrabang, Bangkok 10520, Thailand. ⁶National Institute of Information and Communications Technology, Nukui-Kitamachi 4-2-1, Koganei, Tokyo 184-8795, Japan.

Received: 31 May 2023 Accepted: 21 September 2023

Published: 3 October 2023

References

- Buhari SM, Abdullah M, Yokoyama T, Otsuka Y, Nishioka M, Hasbi AM, Bahari SA, Tsugawa T (2017) Climatology of successive equatorial plasma bubbles observed by GPS ROTI over Malaysia. *J Geophys Res Space Phys* 122:2174–2184. <https://doi.org/10.1002/2016JA023202>
- Bumrungrkit A, Supnithi P, Saito S et al (2022) A study of equatorial plasma bubble structure using VHF radar and GNSS scintillations over the low-latitude regions. *GPS Solut* 26:148. <https://doi.org/10.1007/s10291-022-01321-4>
- Carter BA et al (2014) Geomagnetic control of equatorial plasma bubble activity modeled by the TIEGCM with Kp. *Geophys Res Lett* 41:5331–5339. <https://doi.org/10.1002/2014GL060953>
- Fukao S, Ozawa Y, Yamamoto M, Tsunoda RT (2003) Altitude-extended equatorial spread F observed near sunrise terminator over Indonesia. *Geophys Res Lett* 30:2137. <https://doi.org/10.1029/2003GL018383>
- Gentile LC, Burke WJ, Rich FJ (2006) A global climatology for equatorial plasma bubbles in the topside ionosphere. *Ann Geophys* 24:163–172. <https://doi.org/10.5194/angeo-24-163-2006>
- Hosokawa K, Sakai J, Tomizawa I, Saito S, Tsugawa T, Nishioka M, Ishii M (2020a) A monitoring network for anomalous propagation of aeronautical VHF radio waves due to sporadic E in Japan. *Earth Planets Space* 72:1–10. <https://doi.org/10.1186/s40623-020-01216-z>
- Hosokawa K, Takami K, Saito S et al (2020b) Observations of equatorial plasma bubbles using a low-cost 630.0-nm all-sky imager in Ishigaki Island, Japan. *Earth Planets Space* 72:56. <https://doi.org/10.1186/s40623-020-01187-1>
- Hosokawa K, Kimura K, Sakai J, Saito S, Tomizawa I, Nishioka M, Tsugawa T, Ishii M (2021) Visualizing sporadic E using aeronautical navigation signals at VHF frequencies. *J Space Weather Space Clim*. <https://doi.org/10.1051/swsc/2020075>
- Huang C-S, Kelley MC (1996) Nonlinear evolution of equatorial spread F: 2. Gravity wave seeding of Rayleigh–Taylor instability. *J Geophys Res* 101:293–302
- Kil H (2015) The morphology of equatorial plasma bubbles—a review. *J Astron Space Sci* 32:13–19
- Kil H, Paxton LJ, Oh S-J (2009) Global bubble distribution seen from ROCSAT-1 and its association with the pre-reversal enhancement. *J Geophys Res* 114:A06307. <https://doi.org/10.1029/2008JA013672>
- Kintner PM, Ledvina BM, de Paula ER (2007) GPS and ionospheric scintillations. *Space Weather* 5:S09003. <https://doi.org/10.1029/2006SW000260>
- Kuriki I, Tanohata K, Sakamoto T, Iguchi M (1972) Propagational mode deduced from signal strengths in the VHF band on the trans-equatorial path. *J Radio Res Labs* 19:175–195
- Maruyama T, Kawamura M (2006) Equatorial ionospheric disturbance observed through a transequatorial HF propagation experiment. *Ann Geophys* 24:1401–1409
- Nakata H, Nagashima I, Sakata K, Otsuka Y, Akaike Y, Takano T, Shimakura S, Shiokawa K, Ogawa T (2005) Observations of equatorial plasma bubbles using broadcast VHF radio waves. *Geophys Res Lett* 32:L17110. <https://doi.org/10.1029/2005GL023243>
- Ogawa T, Sagawa E, Otsuka Y et al (2005) Simultaneous ground- and satellite-based airglow observations of geomagnetic conjugate plasma bubbles in the equatorial anomaly. *Earth Planet Space* 57:385–392. <https://doi.org/10.1186/BF03351822>
- Otsuka Y, Shiokawa K, Ogawa T, Wilkinson P (2002) Geomagnetic conjugate observations of equatorial airglow depletions. *Geophys Res Lett* 29:43. <https://doi.org/10.1029/2002GL015347>
- Otsuka Y, Ogawa T, Effendy (2009) VHF radar observations of nighttime F-region field-aligned irregularities over Kototabang, Indonesia. *Earth Planet Space* 61:431–443. <https://doi.org/10.1186/BF03353159>
- Rajesh PK, Lin CH, Chen CH, Chen WH, Lin JT, Chou MY, Chang MT, You CF (2017) Global equatorial plasma bubble growth rates using ionosphere data assimilation. *J Geophys Res Space Phys* 122:3777–3787. <https://doi.org/10.1002/2017JA023968>
- Rao PB, Thome GD (1974) A model for RF scattering from field-aligned heater-induced irregularities. *Radio Sci* 9(11):987–996. <https://doi.org/10.1029/RS009i011p00987>
- Roettger J (1976) The macro-scale structure of equatorial spread-F irregularities. *J Atmos Terr Phys* 38:97–101
- Saito S, Yamamoto M, Maruyama T (2018) Arrival angle and travel time measurements of HF transequatorial propagation for plasma bubble monitoring. *Radio Sci* 53:1304–1315. <https://doi.org/10.1029/2017RS006518>
- Sakai J, Hosokawa K, Tomizawa I, Saito S (2019) A statistical study of anomalous VHF propagation due to the sporadic-E layer in the air-navigation band. *Radio Sci* 54:426–439. <https://doi.org/10.1029/2018RS006781>
- Sakai J, Saito S, Hosokawa K, Tomizawa I (2020) Anomalous propagation of radio waves from distant ILS localizers due to ionospheric sporadic-E. *Space Weather* 18:e2020SW002517. <https://doi.org/10.1029/2020SW002517>
- Shinagawa H, Jin H, Miyoshi Y, Fujiwara H, Yokoyama T, Otsuka Y (2018) Daily and seasonal variations in the linear growth rate of the Rayleigh–Taylor

- instability in the ionosphere obtained with GAIA. *Prog Earth Planet Sci* 5:16
- Shiokawa K, Otsuka Y, Ogawa T, Wilkinson P (2004) Time evolution of high-altitude plasma bubbles imaged at geomagnetic conjugate points. *Ann Geophys* 22:3137–3143
- Sousasantos J, Affonso BJ, Moraes A, Rodrigues FS, Abdu MA, Salles LA, Vani BC (2022) Amplitude scintillation severity and fading profiles under alignment between GPS propagation paths and equatorial plasma bubbles. *Space Weather* 20:e2022SW003243. <https://doi.org/10.1029/2022SW003243>
- Stathacopoulos AD, Barry GH (1974) Geometric considerations in the design of communications circuits using field-aligned ionospheric scatter. *Radio Sci* 9(11):1021–1024. <https://doi.org/10.1029/RS009i011p01021>
- Thébault E, Finlay CC, Beggan CD et al (2015) International geomagnetic reference field: the 12th generation. *Earth Planets Space* 67:79. <https://doi.org/10.1186/s40623-015-0228-9>
- Tsunoda RT (2015) Upwelling: a unit of disturbance in equatorial spread F. *Prog Earth Planet Sci* 2:9. <https://doi.org/10.1186/s40645-015-0038-5>
- Weber EJ, Buchau J, Eather RH, Mende SB (1978) North-south aligned equatorial airglow depletions. *J Geophys Res* 83:712–716
- Woodman RF, LaHoz C (1976) Radar observations of F region equatorial irregularities. *J Geophys Res* 81:5447–5466
- Yokoyama T (2017) A review on the numerical simulation of equatorial plasma bubbles toward scintillation evaluation and forecasting. *Prog Earth Planet Sci* 4:37. <https://doi.org/10.1186/s40645-017-0153-6>

Publisher's Note

Springer Nature remains neutral with regard to jurisdictional claims in published maps and institutional affiliations.

Submit your manuscript to a SpringerOpen[®] journal and benefit from:

- ▶ Convenient online submission
- ▶ Rigorous peer review
- ▶ Open access: articles freely available online
- ▶ High visibility within the field
- ▶ Retaining the copyright to your article

Submit your next manuscript at ▶ [springeropen.com](https://www.springeropen.com)
